

Variation in photoinhibition among *Sasa senanensis*, *Quercus mongolica*, and *Acer mono* in the understory of a deciduous broad-leaved forest exposed to canopy gaps caused by typhoons

Hiroyuki Tobita · Hajime Utsugi · Mitsutoshi Kitao ·
Masazumi Kayama · Akira Uemura · Satoshi Kitaoka ·
Yutaka Maruyama

Received: 18 December 2008 / Revised: 21 October 2009 / Accepted: 26 November 2009 / Published online: 15 December 2009
© Springer-Verlag 2009

Abstract To elucidate mechanisms for tolerating sudden increases in light intensity following canopy gap formation, we investigated susceptibility to photoinhibition in the evergreen clonal plant bamboo, *Sasa senanensis*, and two deciduous broadleaf woody plants, *Quercus mongolica*, and *Acer mono*. We measured pre-dawn photochemical efficiency of photosystem II (F_v/F_m) in plants exposed to canopy gaps and in shade-grown plants through the month following gap formation. Photoinhibition (indicated by decreased F_v/F_m) was smallest in *S. senanensis* and largest in *A. mono*. *S. senanensis* had the highest area-based net CO₂ assimilation rate (A_{area}) and electron transport rate (ETR) under high light conditions. This species also had the highest leaf mass per area (LMA) and leaf nitrogen content per area (N_{area}). Higher values of LMA and N_{area} under shade conditions probably contribute to circumvent photoinhibition through maintenance of a higher ETR capacity. *Q. mongolica*, a gap-dependent species, had properties intermediate between *S. senanensis* and *A. mono*; it appeared less susceptible to photoinhibition than the shade-tolerant *A. mono*. None of the species examined

had increased photosynthetic capacity 1 month after gap formation, indicating that shade-grown leaves were unable to fully acclimate to increased light.

Keywords Acclimation · Chlorophyll fluorescence · Electron transport rate · Leaf mass per area · Net CO₂ assimilation rate

Introduction

The flexibility of responses to modified light environments in windfall areas plays a key role in the competitiveness of understory plants (Percy and Sims 1994; Bazzaz 1996; Krause et al. 2001; Beaudet et al. 2007). Canopy gaps intensify growth competition between regenerating understory plants. To succeed in newly formed gaps, shade-adapted and/or shade-acclimated understory plants must avoid photoinhibition, which is defined as a prolonged decline in photosynthetic light-use efficiency of photosystem (PS) II (Demmig-Adams and Adams 1992; Long et al. 1994), and adapt their photosynthetic apparatus to the increased irradiance.

As typhoons usually hit Japan late in the vegetation period, mature leaves that have developed under shade conditions will be exposed to strong light following windfall events. Such shade-adapted leaves generally have less photoinhibition tolerance and lower photosynthetic acclimation ability to increased light intensities (Osmond 1994; Naidu and DeLucia 1997; Lovelock et al. 1998; Kitao et al. 2000; Yamashita et al. 2000; Oguchi et al. 2005; Wyka et al. 2007) than expanding leaves (Sims and Percy 1992) and leaves developed after windfall gap formation (Kamaluddin and Grace 1992; Percy 1994; Yamashita et al. 2000). Hence, susceptibility to

Communicated by W. Bilger.

H. Tobita (✉) · H. Utsugi · A. Uemura · S. Kitaoka ·
Y. Maruyama
Hokkaido Research Center, Forestry and Forest Products
Research Institute, Sapporo 062-8516, Japan
e-mail: tobi@ffpri.affrc.go.jp

M. Kitao
Forestry and Forest Products Research Institute,
Tsukuba 305-8687, Japan

M. Kayama
Kyusyu Research Center, Forestry and Forest Products Research
Institute, Kurokami 860-0862, Japan

photoinhibition and the ability of mature leaves to adapt to increased irradiation will play a major role in windfall-induced photosynthetic productivity, growth, and competition among understory plants.

Dwarf bamboos (*Sasa*) are common understory plants in temperate and boreal forests of central and northern Asia. In some areas, they severely inhibit regeneration of tree species because of the extreme shading of the forest floor by their 1–3 m high culms that grow clonally at high densities (Nakashizuka 1988; Hiura et al. 1996; Umeki and Kikuzawa 1999; Narukawa and Yamamoto 2002; Takahashi et al. 2003; Noguchi and Yoshida 2004; Abe et al. 2005). Moreover, *Sasa* bamboos indirectly increase seed loss by encouraging development of particularly high rodent densities (Iida 2004).

In our experimental forest, *Sasa senanensis* is one of the dominant components of the understory, which also includes two deciduous woody plants with different regeneration strategies, viz. *Quercus mongolica*, a mid-successional gap-dependent species, and *Acer mono*, a late-successional shade-tolerant species (Koike 1988). *S. senanensis* is capable of significant carbon uptake in late fall and early spring under the leafless canopy in deciduous forests (Lei and Koike 1998). However, it is as yet unclear how the evergreen *S. senanensis* copes with excess light energy following unpredictable windfall events. Species with long-lived leaves are more tolerant of sudden increases in light that occur when tree-fall gaps are formed than shade-acclimated specimens of species with short-lived leaves (Lovell et al. 1998). *S. senanensis* has evergreen leaves that remain functional for several years (Lei and Koike 1998). Field observations show that large canopy gaps formed by typhoons often later develop into open stands with dense *Sasa* undergrowth (Tatewaki 1958). We hypothesized that, in this situation, *S. senanensis* has advantages over broadleaf tree species because of its higher tolerance of sudden increases in light intensity that is attributable to highly efficient energy dissipation mechanisms and a superior ability to acclimatize to increased light. In addition, shade-grown potted seedlings of *Q. mongolica* have higher tolerance to photoinhibition than those of *A. mono* (Kitao et al. 2000, 2006a); this difference, however, has not yet been verified under field conditions.

An opportunity to test our hypothesis arose on 8 September 2004, when the 18th typhoon of the season struck northern Japan. Large canopy gaps were formed in vegetation across Hokkaido, including our experimental deciduous broadleaf forest (Takao et al. 2005). Over several weeks following the event, we studied vulnerabilities to photoinhibition and photosynthetic acclimation ability in *S. senanensis*, *Q. mongolica*, and *A. mono*. To identify factors responsible for different susceptibilities to photoinhibition, we measured pre-dawn photochemical

efficiency of photosystem II (F_v/F_m), photosynthetic properties (CO_2 assimilation and chlorophyll fluorescence) and physiological leaf characters.

Materials and methods

Study site

This study was conducted in a mature secondary deciduous broadleaf forest regenerated after a forest fire in 1912. The site is located in the experimental forest of the Forestry and Forest Products Research Institute, Hokkaido Research Center in Sapporo, Japan (42°59'N, 141°23'E, 180 m above sea level). The topography is rather flat, and the soil type is Andosol (Ishizuka et al. 2006). The mean annual temperature is 7.1°C (1981–2000) and the mean annual precipitation is 957 mm. Snow accumulation is about 1 m from mid-November to mid-April. The dominant canopy tree species is *Betula platyphylla* Sukatch. var. *japonica* (Miq.) Hara. Mean tree height of this birch is 18.3 m and mean stem diameter at 1.3 m above ground is 0.23 m (Utsugi et al. 2005). In the study site, a 0.25 ha study plot (50 m × 50 m) had been established in previous work for measurement of tree growth, and 100 quadrats (2 m × 2 m) had been deployed within the plot to monitor survival and growth rates of tree seedlings (Abe et al. 2003). At the site, *S. senanensis* underwent a mass flowering before numerous patches died off in 1995. Thereafter, the *S. senanensis* population regained size through vegetative spreading, but has not yet recovered its original density (Abe et al. 2003). When understory bamboo density was low, seedlings of broadleaf tree species sprouted up, but most were still shorter (average height ± SE; 0.24 ± 0.01 and 0.14 ± 0.03 m, for *Q. mongolica* and *A. mono*, respectively) in September 2004 than regenerated *S. senanensis* (0.49 ± 0.01 m).

Plant materials

We examined understory plants of *S. senanensis* (Fr. & Sav.) Rehd, and two broadleaf tree species, *Q. mongolica* var. *grosseserrata* Blume and *A. mono* Maxim. var. *glabrum* (Lév. & Van't.) Hara. The broadleaf tree individuals studied were not directly beneath neighboring culms of *S. senanensis*. *S. senanensis* is monocarpic, with a regeneration interval of >60 years, but usually forms dense stands by clonal growth and often reaches 100% cover in the understory (Hiura et al. 1996). The average height reaches about 1 m in the forest understory. *Q. mongolica* is a major canopy constituent of mature mixed forests in the cool temperate region of northern Japan (Koike 1988; Takahashi et al. 2003). *A. mono* is capable of persisting in the forest understory for most of its life (Koike 1988).

On 8 September 2004, more than 50% of the crown area at the site was destroyed by a typhoon (Takao et al. 2005); the canopy was closed before the typhoon. Three 2×2 m plots located under newly formed gaps were selected for study (“gap plots”). Each included all three experimental species, viz. *S. senanensis* (total number of plants analyzed in the three squares: $n = 13$), *Q. mongolica* ($n = 13$), and *A. mono* ($n = 16$) (“gap plants”; one leaf per plant). One 2×2 m plot that had not been affected by the typhoon (“shade plot”) was selected as a control. It included six plants of all three experimental species (“shade plants”; one leaf per plant). In these “gap plots” and “shade plots”, we selected for physiological measurements saplings of *Q. mongolica* and *A. mono* that were not suppressed by *S. senanensis* or other understory species. We examined mature leaves of *Q. mongolica* and *A. mono* that had started to unfold in mid-May of the same year, whereas in *S. senanensis*, we studied the third leaves (counted from the shoot apex) that had started to develop in early July.

We measured photosynthetic photon flux density (PPFD) above the crown layer of understory *S. senanensis* in the three experimental “gap plots” using PPFD sensors (LI-190SA, Li-Cor, NE, USA) at Day 6 after the typhoon. These measurements were made under overcast skies. At the same time, we also measured PPFD above the canopy of dominant trees in this area. Relative PPFD (rPPFD), i.e. understory PPFD divided by above-canopy PPFD, was calculated for each plot as the mean of 120 measurements taken at 1 s intervals. In the present study, rPPFD was used as a measure of the growth light environment in the forest understory.

Photoinhibition following canopy gap formation

To evaluate the extent of photoinhibition caused by increased irradiance following the disturbance, we determined initial (F_0) and maximum fluorescence (F_m) after an overnight dark-adaptation for all “gap plants” in three “gap plots” (one leaf per plant), using a portable fluorometer (PAM-2000, Walz, Effeltrich, Germany) at a saturating PPFD of $7,000 \mu\text{mol m}^{-2} \text{s}^{-1}$ for 1 s to obtain F_m . The ratio of variable to maximum fluorescence (F_v/F_m where $F_v = F_m - F_0$) represents maximum PS II photochemical efficiency (Schreiber et al. 1994). Measurements were conducted from Day 4 to Day 31 after the typhoon. F_v/F_m was also measured in “shade plants” as controls from Day 16 to Day 31.

Photosynthetic properties of “shade plants” on Days 19–21 after the typhoon

CO_2 assimilation rate and chlorophyll fluorescence were measured simultaneously in situ in four “shade plant” mature leaves of each species (one leaf per plant) using a

leaf chamber fluorometer (LI-6400-40, Li-Cor) connected to a portable photosynthesis system (LI-6400, Li-Cor) on Days 19–21 after the typhoon. Light-dependent net CO_2 assimilation rate per leaf area (A_{area}), quantum yield of PS II electron transport (Φ_{PSII}), photochemical quenching (q_p), and photochemical efficiency of open PS II (F'_v/F'_m) were determined at photosynthetic steady state under actual CO_2 concentration of $360 \mu\text{mol mol}^{-1}$ and 11 levels of PPFD (2,000, 1,600, 1,200, 800, 600, 400, 250, 160, 80, 40, and $0 \mu\text{mol m}^{-2} \text{s}^{-1}$). Using fluorescence yield under photosynthetic steady state, F_s , and maximum fluorescence, F'_m determined at saturating light for 1 s, we calculated $\Phi_{\text{PSII}} (= (F'_m - F_s)/F'_m)$ (Genty et al. 1989). To determine minimum fluorescence, F'_0 , far-red light was applied after turning off the actinic light. F'_0 was used to derive $q_p (= (F'_m - F_s)/(F'_m - F'_0))$ and $F'_v/F'_m (= (F'_m - F'_0)/F'_m)$, calculated according to Schreiber et al. (1994). Leaf temperature was maintained at $22\text{--}23^\circ\text{C}$, and leaf to air vapor pressure difference was kept at <1.2 kPa. Electron transport rate (ETR) was calculated as $\text{ETR} = 0.5 \times \Phi_{\text{PSII}} \times \text{leaf absorptance} \times \text{incident PPFD}$. Absorptances at 400–700 nm of the leaves used for measurements of photosynthetic properties were determined with a spectroradiometer (LI-1800C, Li-Cor) and an external-integrating sphere (LI-1800-12S, Li-Cor). Partitioning of absorbed light energy among various pathways was estimated using the model proposed by Demmig-Adams et al. (1996). This method is based on a “puddle” model assuming limited connectivity between the PS II complexes. In this model, the light energy sink comprises three parts: photosynthetic electron transport defined by Φ_{PSII} , heat dissipation, and excess energy. Heat dissipation reduces F'_v/F'_m (Demmig-Adams et al. 1995; Gilmore and Björkman 1995) and is defined as $1 - F'_v/F'_m$. Energy that is neither consumed for electron transport nor dissipated as heat is defined as excess energy (E), $E = F'_v/F'_m \times (1 - q_p)$ (Demmig-Adams et al. 1996). The absolute value of excess energy was calculated as $E \times \text{leaf absorptance} \times \text{incident PPFD} \times 0.5$ (Kato et al. 2003).

Before measuring light-dependency of photosynthesis in the same leaves, we measured A_{area} and chlorophyll fluorescence at $600 \mu\text{mol m}^{-2} \text{s}^{-1}$ PPFD simultaneously in situ at four levels of CO_2 concentration (360, 200, 100, and $1,500 \mu\text{mol mol}^{-1}$). We assumed that $600 \mu\text{mol m}^{-2} \text{s}^{-1}$ PPFD established light-saturated conditions for “shade plants”. Apparent carboxylation efficiency (CE) was derived from the initial slope of the relationship between intercellular CO_2 concentration (C_i) and A_{area} below C_i of $300 \mu\text{mol mol}^{-1}$ using linear regression on the basis of A_{area} measured at actual CO_2 of 360, 200, 100 $\mu\text{mol mol}^{-1}$. The A_{area} measured at actual CO_2 of $1,500 \mu\text{mol mol}^{-1}$ was used as maximum photosynthetic rate (A_{max}). Leaf area-based CO_2 assimilation rate ($A_{\text{area-600}}$) and leaf mass-

based CO_2 assimilation rate ($A_{\text{mass-600}}$), transpiration rate ($T_{\text{r-600}}$), instantaneous water-use efficiency (WUE; $A_{\text{area-600}}$ per $T_{\text{r-600}}$), photosynthetic nitrogen-use efficiency [PNUE; $A_{\text{area-600}}$ per area-based leaf nitrogen content (N_{area})], and chlorophyll fluorescence parameters (ETR_{600} , $q_{\text{P-600}}$, and $F'_v/F'_{\text{m-600}}$) were determined for $600 \mu\text{mol m}^{-2} \text{s}^{-1}$ PPFD at $360 \mu\text{mol mol}^{-1} \text{CO}_2$ for each leaf.

Photosynthetic properties of “shade plants” and “gap plants” about 1 month after the disturbance

About 1 month after the typhoon, A_{area} and chlorophyll fluorescence at $600 \mu\text{mol m}^{-2} \text{s}^{-1}$ PPFD were measured at $360 \mu\text{mol mol}^{-1} \text{CO}_2$ in four mature leaves of “shade plants” (one leaf per plant, Day 34) and in five mature leaves of “gap plants” (one leaf per plant, Day 31) of the three species. The five “gap plants” were selected from two plots within the three “gap plots”. In addition, for this measurement, leaf absorptance was derived using a calibration curve plot of SPAD readings (measured using a SPAD chlorophyll meter, SPAD 502, Minolta, Osaka, Japan) and leaf absorptance for the three species measured on Days 19–21. Because there was little difference among species in the relationships between SPAD readings and leaf absorptance, we used the same equation for all species. The equation was:

$$\begin{aligned} \text{Leaf absorptance} &= 0.200 \times \ln[\text{SPAD reading}] \\ &+ 0.129(n = 12, R^2 = 0.972, \\ &P < 0.05). \end{aligned}$$

Leaf characters

All the leaves used for measurements of photosynthetic properties (Days 19–21 and Day 34 in “shade plants” and Day 31 in “gap plants”) were dried to constant weight at 80°C and were then used for the determination of leaf mass per area (LMA) and N_{area} . Mass-based leaf N content (N_{mass}) was determined with a combustion method using an NC-analyzer (SUMIGRAPH NC-800, Sumika, Osaka, Japan). SPAD readings were obtained using a SPAD chlorophyll meter, which has a close correlation with chlorophyll content (Markwell et al. 1995; Uddling et al. 2007). Leaf thickness was measured using a digimatic micrometer (MDC-25M, Mitutoyo, Kanagawa, Japan).

Statistical analysis

Split-plot analysis of variance was used to compare F_v/F_m between species in all three gap plots (“gap plants”). Analysis of variance was used to compare light-dependent photosynthetic properties and leaf characters of “shade plants” (Days 19–21) between species. Statistical

significance of differences between pairs of species was tested with the Tukey–Kramer post hoc test at a probability level $P < 0.05$ using JMP (SAS Institute 2003). Statistical significance of differences between F_v/F_m values determined at different times, and between “shade plants” and “gap plants” were tested using Student’s t test ($P < 0.05$). Statistical significance of differences about 1 month after the typhoon between “shade plants” (Day 34) and “gap plants” (Day 31) in photosynthetic properties under saturating light (PPFD = $600 \mu\text{mol m}^{-2} \text{s}^{-1}$) and leaf characters were tested using Student’s t test ($P < 0.05$).

Results

“Shade plant” chlorophyll fluorescence light response curves on Days 19–21 after the typhoon

Above $160 \mu\text{mol m}^{-2} \text{s}^{-1}$ PPFD, light-dependent ETR in “shade plants” on Days 19–21 was highest in *S. senanensis* and lowest in *A. mono* ($P < 0.05$; Fig. 1a). ETR values reached maxima at PPFDs of around 400, 250, and $80 \mu\text{mol m}^{-2} \text{s}^{-1}$ in *S. senanensis*, *Q. mongolica*, and *A. mono*, respectively. q_{P} , which represents the openness of PS II centers (Krause and Weis 1991; Schreiber et al. 1994), decreased in all species as light intensity increased, most markedly in *A. mono* and least in *S. senanensis* (Fig. 1b). As a result, *A. mono* had the lowest q_{P} above $80 \mu\text{mol m}^{-2} \text{s}^{-1}$ PPFD, whereas *S. senanensis* had the highest above $400 \mu\text{mol m}^{-2} \text{s}^{-1}$ PPFD ($P < 0.05$). F'_v/F'_m , which represents the efficiency of open PS II energy conversion (Schreiber et al. 1994), also declined with increasing incident PPFD, and this decrease occurred at a lower PPFD in *A. mono* than in *Q. mongolica* and *S. senanensis* (Fig. 1c). F'_v/F'_m reached minimum levels at PPFDs of around 1,200, 600, and $160 \mu\text{mol m}^{-2} \text{s}^{-1}$ in *S. senanensis*, *Q. mongolica*, and *A. mono*, respectively. In contrast to q_{P} , F'_v/F'_m above $1,200 \mu\text{mol m}^{-2} \text{s}^{-1}$ PPFD was lowest in *S. senanensis* ($P < 0.05$). The absolute value of the excess energy, which was estimated with the model of Demmig-Adams et al. (1996), increased in all species as the absorbed light intensity increased (Fig. 2). At a given absorbed PPFD, *A. mono* had the largest excess energy followed by *Q. mongolica* and *S. senanensis* ($P < 0.05$).

Gas exchange of “shade plants” on Days 19–21 after the typhoon

The light-dependent A_{area} of “shade plants” on Days 19–21 tracked trends similar to ETR: above $80 \mu\text{mol m}^{-2} \text{s}^{-1}$ PPFD, *S. senanensis* had the highest A_{area} followed by *Q. mongolica* and *A. mono* ($P < 0.05$; Fig. 3). *S. senanensis* had the highest $A_{\text{area-600}}$, A_{max} , and CE among the

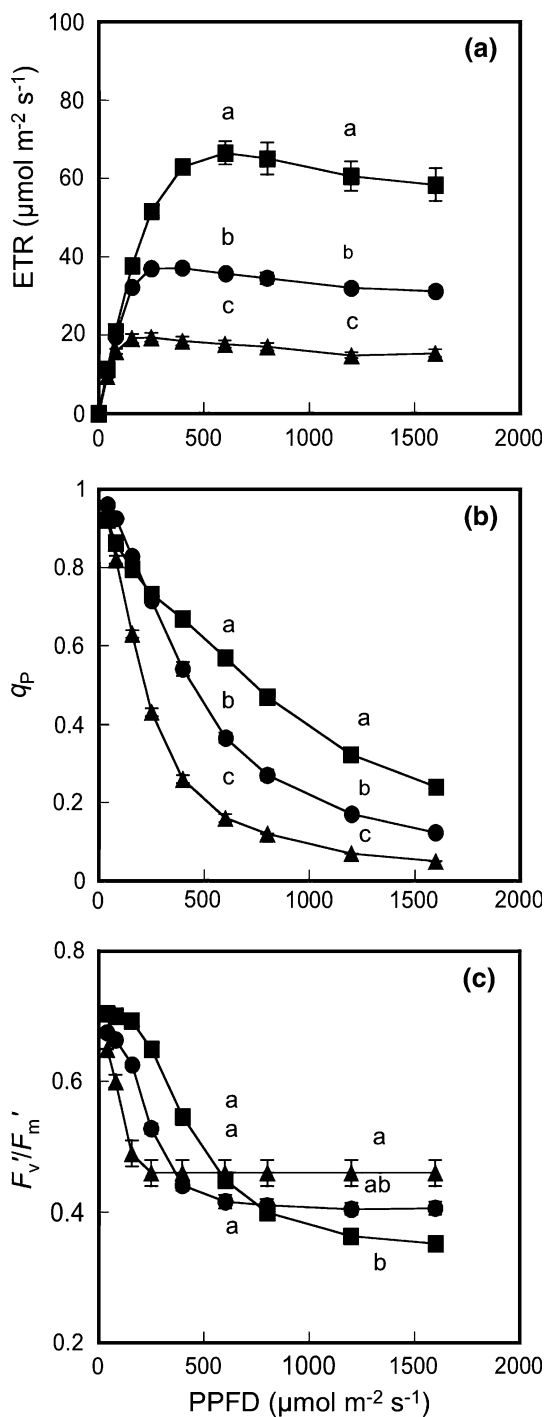


Fig. 1 Responses of electron transport rate (ETR) (a), photochemical quenching (q_p) (b), the efficiency of energy conversion of open PS II (F_v'/F_m') (c) to incident photon flux density (PPFD) in “shade plants” of *S. senanensis* (squares), *Q. mongolica* (circles), *A. mono* (triangles). Data for light–response curves shown were obtained on Days 19–21 after the typhoon; values are means \pm SE ($n = 4$). Different letters at 600 and 1,200 $\mu\text{mol m}^{-2} \text{s}^{-1}$ PPFD indicate statistically significant differences between species at $P < 0.05$ (Tukey–Kramer test)

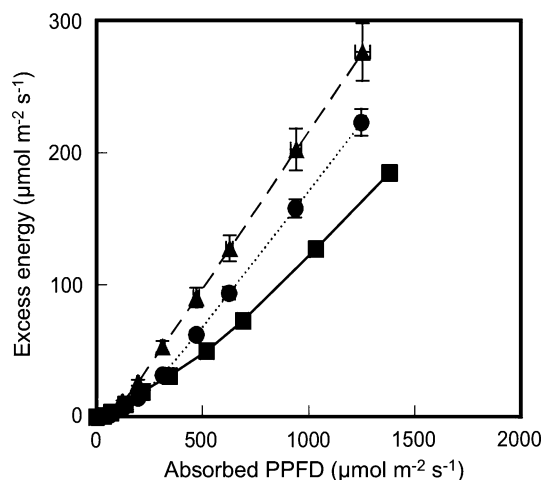


Fig. 2 Relationships between the rate of excess light energy estimated from: [excess energy (E) \times leaf absorbance \times incident PPFD \times 0.5] and absorbed PPFD for “shade plants” on Days 19–21 of *S. senanensis* (squares, solid line), *Q. mongolica* (circles, dotted line), *A. mono* (triangles, dashed line). Values are means \pm SE ($n = 4$)

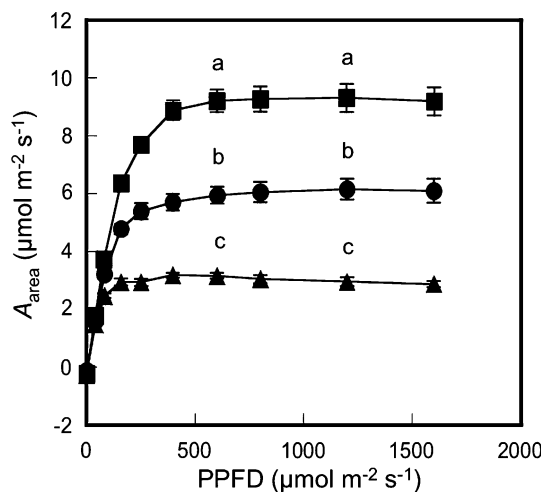


Fig. 3 Response of leaf area-based net CO_2 assimilation rate (A_{area}) to incident photon flux density (PPFD) in “shade plants” of *S. senanensis* (squares), *Q. mongolica* (circles), *A. mono* (triangles). Light–response curves were measured on Days 19–21 after the typhoon; values are means \pm SE ($n = 4$). Different letters at 600 and 1,200 $\mu\text{mol m}^{-2} \text{s}^{-1}$ PPFD indicate statistically significant differences between species at $P < 0.05$ (Tukey–Kramer test)

three species ($P < 0.05$; Table 1). *S. senanensis* also had the highest WUE, followed by *A. mono* and *Q. mongolica* ($P < 0.05$). $A_{\text{mass-600}}$ and PNUE were highest in leaves of *Q. mongolica* ($P < 0.05$). R_d was not significantly different among species.

Table 1 Photosynthetic parameters at 600 $\mu\text{mol m}^{-2} \text{s}^{-1}$ PPFD and 360 $\mu\text{mol mol}^{-1} \text{CO}_2$ and dark respiration (R_d) on Days 19–21 after the typhoon in “shade plants” of *S. senanensis*, *Q. mongolica*, and *A. mono*

	<i>Sasa senanensis</i>	<i>Quercus mongolica</i>	<i>Acer mono</i>
Area-based photosynthetic rate $A_{\text{area-600}}$ ($\mu\text{mol m}^{-2} \text{s}^{-1}$)	7.48 \pm 0.38 a	6.10 \pm 0.29 b	2.94 \pm 0.07 c
Mass-based photosynthetic rate $A_{\text{mass-600}}$ ($\text{nmol g}^{-1} \text{s}^{-1}$)	113.85 \pm 9.27 b	181.91 \pm 8.92 a	128.84 \pm 8.94 b
Maximum photosynthetic rate A_{max} ($\mu\text{mol m}^{-2} \text{s}^{-1}$)	19.54 \pm 0.61 a	12.18 \pm 0.59 b	8.42 \pm 0.26 c
Apparent carboxylation efficiency, CE ($\mu\text{mol m}^{-2} \text{s}^{-1}$)	0.069 \pm 0.003 a	0.033 \pm 0.003 b	0.024 \pm 0.002 b
Photosynthetic nitrogen-use efficiency, PNUE ($\mu\text{mol g}^{-1} \text{s}^{-1}$)	5.09 \pm 0.32 b	8.01 \pm 0.78 a	6.44 \pm 0.77 ab
Transpiration rate, $T_{\text{r-600}}$ ($\text{mmol m}^{-2} \text{s}^{-1}$)	0.72 \pm 0.05 b	1.14 \pm 0.06 a	0.41 \pm 0.03 c
Water-use efficiency, WUE	10.40 \pm 0.36 a	5.39 \pm 0.18 c	7.27 \pm 0.58 b
Dark respiration, R_d ($\mu\text{mol m}^{-2} \text{s}^{-1}$)	0.18 \pm 0.02 a	0.23 \pm 0.10 a	0.18 \pm 0.05 a

The values are mean \pm SE ($n = 4$). Different lower case letters indicate statistically significant differences between species at $P < 0.05$ (Tukey–Kramer test)

“Shade plant” leaf characters on Days 19–21 after the typhoon

On Days 19–21 after the typhoon, “shade plants” of *S. senanensis* had the largest LMA and leaf thickness, the highest N_{area} and chlorophyll content (SPAD reading), and the greatest leaf absorptance among the three species examined ($P < 0.05$; Table 2). On the other hand, N_{mass} was not different among species. “Shade plants” of *Q. mongolica* had larger LMA and higher N_{area} than those of *A. mono* ($P < 0.05$).

“Gap plant” F_v/F_m after the typhoon

Before the typhoon of September 8, relative PPFD (rPPFD) above the crown layer of *S. senanensis* was 5–6% of full sunlight (Utsugi, personal communications). After the typhoon, the corresponding rPPFD in the “gap plots” was 63 \pm 5% (mean \pm SE of the 3 experimental plots). This value of rPPFD corresponds approximately to the light condition before the bud burst in this deciduous forest with closed canopy until the disturbance (Tobita et al. 2002). “Shade plants” had an $F_v/F_m \geq 0.8$ on Day 16 after the typhoon (*S. senanensis* 0.819 \pm 0.001, *Q. mongolica* 0.815 \pm 0.003, *A. mono* 0.802 \pm 0.002; mean \pm SE)

(Fig. 4). F_v/F_m of “shade plants” did not change from Days 16 to 31 after the typhoon. We had not measured F_v/F_m of “gap plants” and “shade plants” before the typhoon. However, F_v/F_m of “shade plants” may be used to represent typical pre-windfall values. On Day 4 after the creation of canopy gaps by the typhoon, “gap plant” F_v/F_m decreased significantly compared to the pre-windfall values in all three species. *S. senanensis* had the highest F_v/F_m , followed by *Q. mongolica* and *A. mono* ($P < 0.05$; Fig. 4). Though predawn F_v/F_m values of “gap plants” of all species did recover slowly from Days 4 to 31, they had not reached “shade plant” levels by Day 31 ($P < 0.05$; Fig. 4). “Gap plants” of *S. senanensis* and *Q. mongolica* had 91 \pm 1% and 88 \pm 1% recoveries of initial values (mean \pm SE), respectively. The recovery ratio was lowest in “gap plants” of *A. mono* (77 \pm 2%), and a fraction of the leaves in this species turned yellow and died off within a month of gap formation.

“Shade plant” and “gap plant” chlorophyll fluorescence about 1 month after the typhoon

“Shade plant” ETR_{600} , $q_{\text{P-600}}$, and $F'_v/F'_{\text{m-600}}$ values of all species did not change significantly from Days 19–21 to Day 34, except for an increase in *S. senanensis* $q_{\text{P-600}}$

Table 2 Leaf characters of “shade plants” of *S. senanensis*, *Q. mongolica*, and *A. mono* on Days 19–21 after the typhoon

	<i>Sasa senanensis</i>	<i>Quercus mongolica</i>	<i>Acer mono</i>
Leaf mass per area, LMA (g m^{-2})	66.49 \pm 4.48 a	33.54 \pm 0.26 b	23.00 \pm 1.02 c
Leaf thickness (mm)	0.174 \pm 0.003 a	0.108 \pm 0.002 b	0.098 \pm 0.003 b
Leaf nitrogen per mass, N_{mass} (mg g^{-1})	22.32 \pm 0.85 a	23.07 \pm 1.31 a	20.39 \pm 1.24 a
Leaf nitrogen per area N_{area} (g m^{-2})	1.47 \pm 0.05 a	0.77 \pm 0.05 b	0.47 \pm 0.05 c
Chlorophyll content, SPAD reading	39.18 \pm 1.30 a	26.98 \pm 1.46 b	25.70 \pm 2.49 b
Leaf absorptance	0.86 \pm 0.01 a	0.78 \pm 0.01 b	0.78 \pm 0.02 b

The values are mean \pm SE ($n = 4$). Different lower case letters indicate statistically significant differences between species at $P < 0.05$ (Tukey–Kramer test)

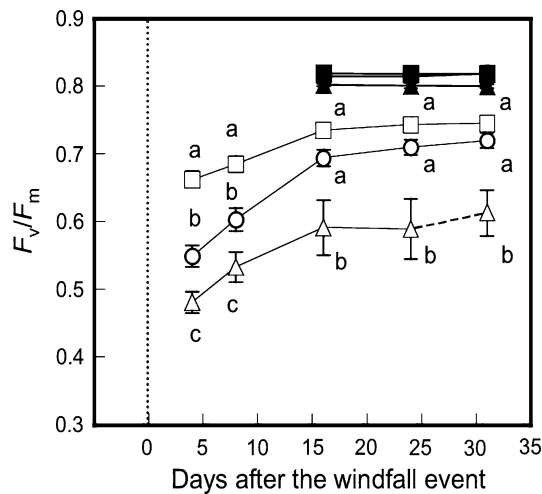


Fig. 4 Pre-dawn maximum photochemical efficiency of PS II (F_v/F_m) in “shade plants” (closed symbols) and “gap plants” (open symbols) of *S. senanensis* (squares), *Q. mongolica* (circles), and *A. mono* (triangles) following canopy gap formation by a typhoon. Values are means \pm SE of “shade plants” ($n = 6$) and “gap plants” (*S. senanensis*: $n = 13$, *Q. mongolica*: $n = 13$, *A. mono*: $n = 16$). Different letters indicate statistically significant differences between species in “gap plants” at $P < 0.05$ (Tukey–Kramer test). The “gap plant” value on Day 31 for *A. mono* is the average value except for two fallen leaves after Day 24. For this reason, points are joined by a dashed line

(0.52 ± 0.04 on Days 19–21) and a decrease in *Q. mongolica* F'_v/F'_{m-600} (0.46 ± 0.01 on Days 19–21) ($P < 0.05$; Fig. 5). “Gap plants” and “shade plants” of *S. senanensis* were not significantly different in ETR_{600} , q_{P-600} , or F'_v/F'_{m-600} at about 1 month after the typhoon (Fig. 5), whereas “gap plants” of *Q. mongolica* and *A. mono* had significantly higher q_{P-600} values than “shade plants” at that time ($P < 0.05$; Fig. 5b). In addition, F'_v/F'_{m-600} values of *A. mono* “gap plants” were significantly lower than those of “shade plants” (Fig. 5c). Though ETR_{600} and q_{P-600} were highest in “gap plants” of *S. senanensis* among three species, F'_v/F'_{m-600} values of “gap plants” were not significantly different among species. The absolute excess energy values at incident $600 \mu\text{mol m}^{-2} \text{s}^{-1}$ PPFD was lower in “gap plants” than in “shade plants” of *A. mono* and *Q. mongolica*, but not in *S. senanensis*, although the absorbed light intensity was not the same between “shade plants” and “gap plants” (Fig. 6). As a result, “gap plants” of *A. mono* and *Q. mongolica* had relationships between absorbed light and excess energy similar to that of *S. senanensis* “shade plants”.

Gas exchange in “shade plants” and “gap plants” about 1 month after the typhoon

For all species, there were no significant changes in “shade plant” gas exchange parameters from Days 19–21 to Day

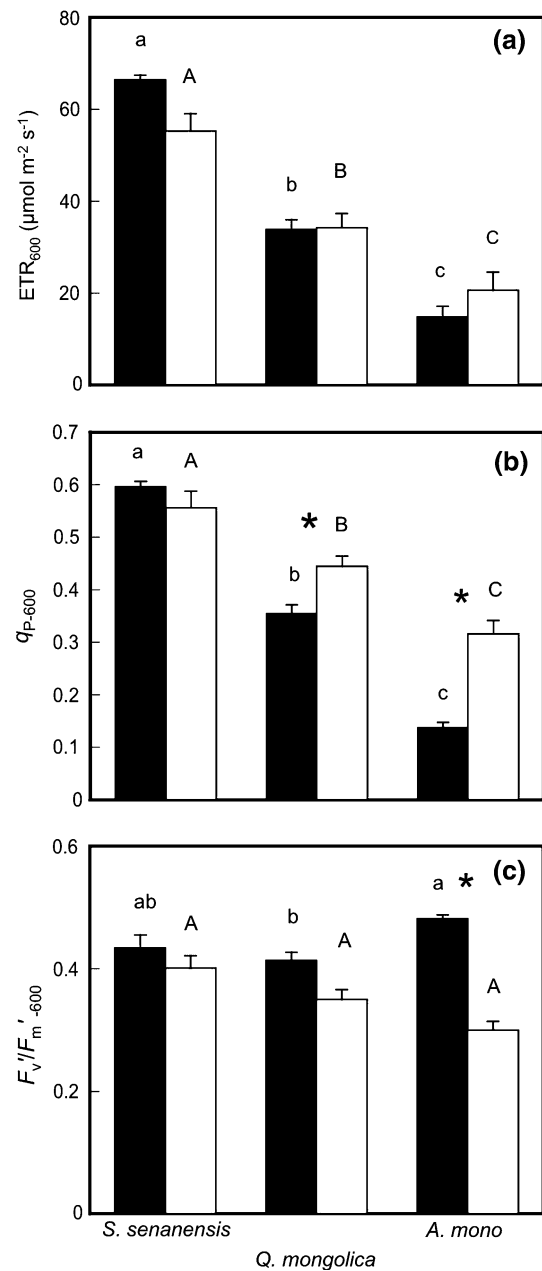


Fig. 5 Electron transport rate (ETR_{600}) (a), photochemical quenching (q_{P-600}) (b), and the efficiency of energy conversion of open PS II (F'_v/F'_{m-600}) (c) at $600 \mu\text{mol m}^{-2} \text{s}^{-1}$ PPFD and $360 \mu\text{mol mol}^{-1}$ CO_2 concentration in “shade plants” on Day 34 (closed bars) and “gap plants” on Day 31 (open bars) of *S. senanensis*, *Q. mongolica*, and *A. mono*. Values are means \pm SE ($n = 4$ on Day 34, $n = 5$ on Day 31). Different letters indicate statistically significant differences between species at $P < 0.05$ (Tukey–Kramer test). “Asterisk” indicates statistically significant differences between “shade plants” (Day 34) and “gap plants” (Day 31) in a given species at $P < 0.05$ (Student’s t test)

34 after the typhoon, except for a decrease in T_{r-600} and an increase in WUE in *Q. mongolica* (Table 1; Fig. 7). “Gap plant” $A_{\text{area-600}}$ and $A_{\text{mass-600}}$ values were not different from those of “shade plants” in any species at about 1 month

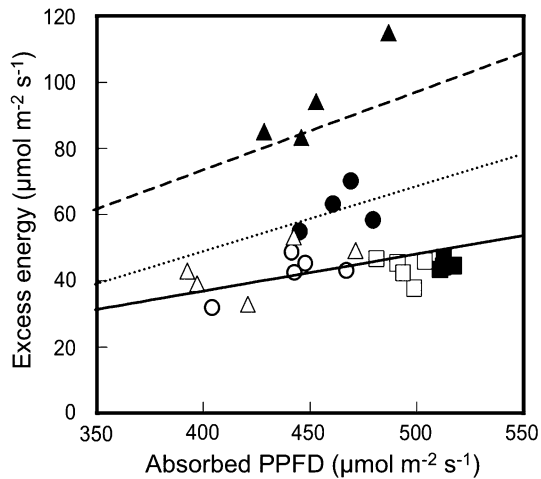
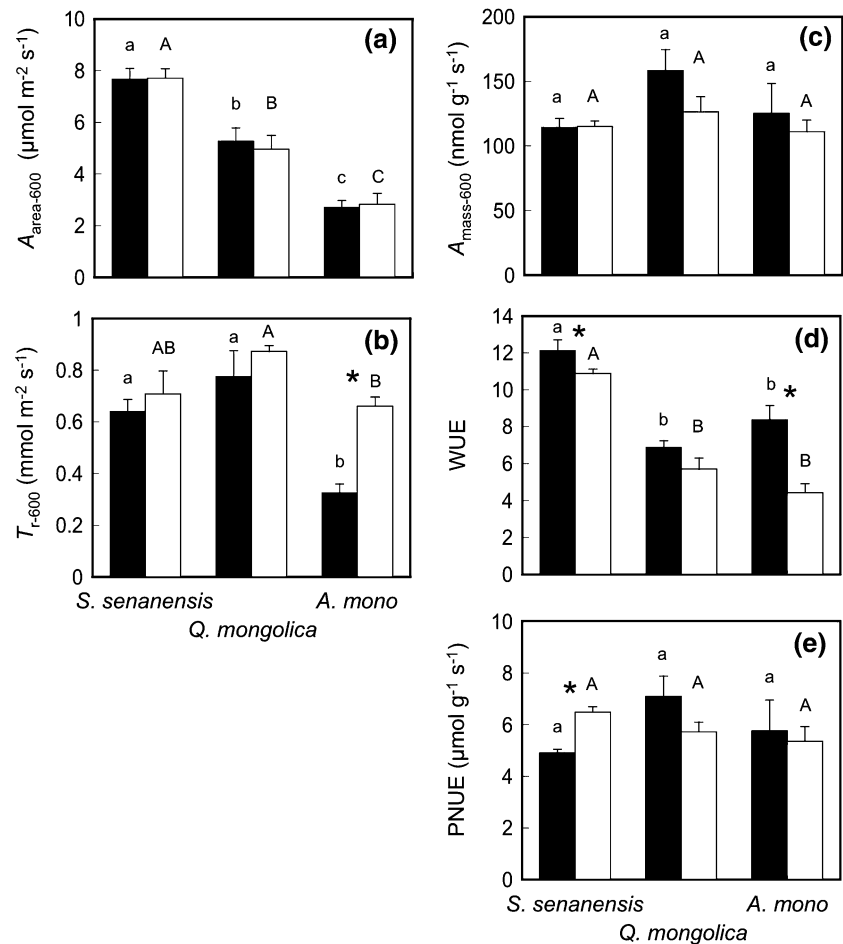


Fig. 6 Relationship between the rate of excess light energy estimated from: [$\text{excess energy } (E) \times \text{leaf absorptance} \times \text{incident PPFD} \times 0.5$] and absorbed PPFD in “shade plants” on Day 34 (closed symbols) and “gap plants” on Day 31 (open symbols) of *S. senanensis* (squares), *Q. mongolica* (circles), and *A. mono* (triangles). Three curves shown present data from Fig. 2 for “shade plants” of *S. senanensis* (solid line), *Q. mongolica* (dotted line), *A. mono* (dashed line)

Fig. 7 Area-based net CO₂ assimilation rate ($A_{\text{area-600}}$) (a), transpiration rate ($T_{\text{r-600}}$) (b), mass-based net CO₂ assimilation rate ($A_{\text{mass-600}}$) (c), instantaneous water-use efficiency (WUE) (d), and photosynthetic nitrogen-use efficiency (PNUE) (e) at 600 $\mu\text{mol m}^{-2} \text{s}^{-1}$ PPFD and 360 $\mu\text{mol mol}^{-1}$ CO₂ concentration in “shade plants” on Day 34 (closed bars), and “gap plants” on Day 31 (open bars) of *S. senanensis*, *Q. mongolica*, and *A. mono*. Values are means \pm SE ($n = 4$ on Day 34, $n = 5$ on Day 31). Different letters indicate statistically significant differences between species at $P < 0.05$ (Tukey–Kramer test). “Asterisk” indicates statistically significant differences between “shade plants” (Day 34) and “gap plants” (Day 31) in a given species at $P < 0.05$ (Student’s t test)



after the typhoon (Fig. 7a, c). “Gap plants” of *S. senanensis*, however, had significantly lower WUE values than those of “shade plants” ($P < 0.05$; Fig. 7d). “Gap plants” of *A. mono* had significantly higher $T_{\text{r-600}}$ values and lower WUE values than shade plants of the same species ($P < 0.05$; Fig. 7b, d). PNUE was significantly higher in “gap plants” than in “shade plants” of *S. senanensis* ($P < 0.05$), but the difference was not significant in the other two species (Fig. 7e).

Leaf characters of “shade plants” and “gap plants” about 1 month after the typhoon

Leaf characters of “shade plants” of all three species did not change over the time period from Days 19–21 to Day 34 after the typhoon (Table 2; Fig. 8). At about 1 month after the typhoon, LMA of “gap plants” increased significantly above that of “shade plants” in only *Q. mongolica* ($P < 0.05$; Fig. 8a). Though N_{area} did not differ significantly between “shade plants” and “gap plants” of *Q. mongolica* and *A. mono* (Fig. 8b), the “gap plant” value

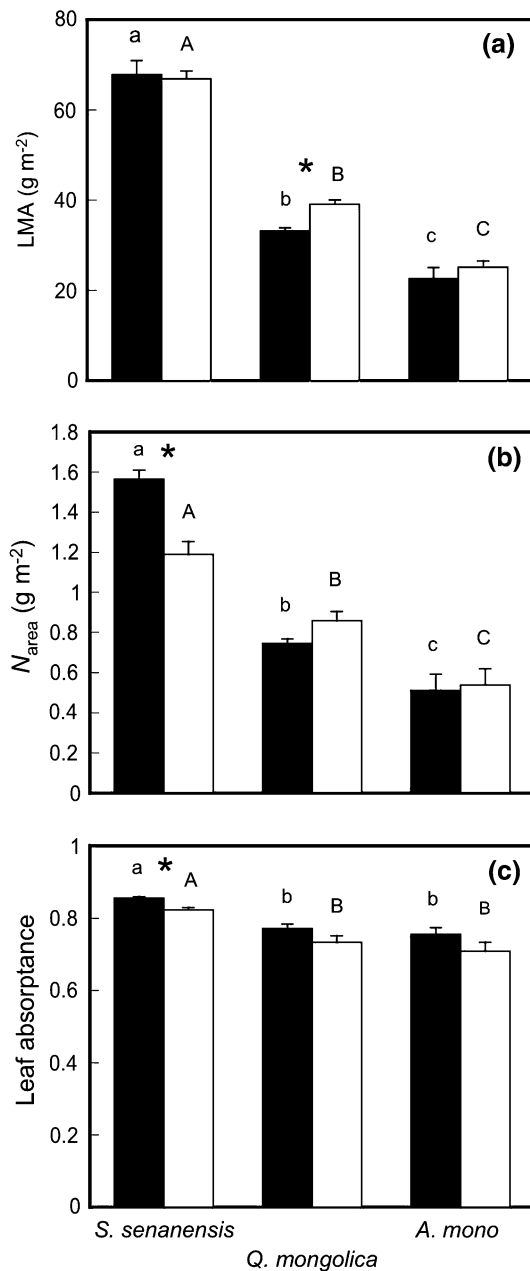


Fig. 8 Leaf mass per unit leaf area (LMA) (a), area-based leaf nitrogen content (N_{area}) (b), and light absorbance of leaves (c) in “shade plants” on Day 34 (closed bars) and “gap plants” on Day 31 (open bars) of *S. senanensis*, *Q. mongolica*, and *A. mono*. Values shown are means \pm SE ($n = 4$ on Day 34, $n = 5$ on Day 31). Different letters indicate statistically significant differences between species at $P < 0.05$ (Tukey–Kramer test). “Asterisk” indicates statistically significant differences between “shade plants” (Day 34) and “gap plants” (Day 31) in a given species at $P < 0.05$ (Student’s *t* test)

for *S. senanensis* was significantly lower than that of “shade plants” ($P < 0.05$). In *S. senanensis*, leaf light absorbance of “gap plants” was significantly lower than that of “shade plants” (Fig. 8c).

Discussion

Initial decline and subsequent recovery of F_v/F_m in *S. senanensis* following exposure to increased irradiance in forest gaps (newly created by a typhoon) showed that this species had the lowest degree of photoinhibition among those tested (Fig. 4) (Krause 1994; Krause et al. 1995; Kitao et al. 2000). A decrease in overnight dark-adapted F_v/F_m is generally used as a measure of photoinhibition (Ögren 1994; Krause et al. 1995). Severity of photoinhibition is determined by both damage and protective processes in PS II indicated by the recovery of F_v/F_m (Yamashita et al. 2000; Shimizu et al. 2006). We suggest that the rapid decrease in F_v/F_m of “gap plants” compared to “shade plants” on Day 16 following gap formation indicates the onset of photodamage to PS II (i.e. number of closed PS II centers increases). F_0 is thought to reflect the size of the antenna chlorophyll and the magnitude of inhibited PS II centers (Krause and Weis 1991). The pattern of change in F_0 represents the different processes of photoinactivation and restoration of PS II (Krause and Weis 1991). In our study, although there were no F_0 data for the first 4 days after gap formation, F_0 of “gap plants” tended to increase gradually from Day 4 to Day 31 in all species (data not shown). In the period from Day 4 to Day 31, F_v/F_m (and F_0) increased in all species (Fig. 4), suggesting an increase in the number of open PS II centers and probably a replacement through synthesis of the damaged D1 proteins (Leitsch et al. 1994; Thiele et al. 1996). In this phase, there may be a gradual recovery from photodamage as the process of photoprotection becomes established in the leaves (Thiele et al. 1996). However, full recovery was not achieved in all species, notably in *A. mono* (Fig. 4).

Leaf-level avoidance of high light stress can be attributed to a variety of physiological processes (Lovelock et al. 1998). Energy consumption via photosynthetic electron transport connected to PS II is an important factor in photoinhibition avoidance (Öquist et al. 1993; Baroli and Melis 1998; Kitao et al. 2003, 2006b). In the present study, species with higher ETR capacity (Fig. 1a) had lower levels of photoinhibition, as indicated by a reduced transient decline in predawn F_v/F_m following gap formation (Fig. 4). Thus, a higher ETR in shade-grown plants (Fig. 1a; *S. senanensis* > *Q. mongolica* > *A. mono*) might explain the different levels of photoinhibition detected (Fig. 4). In addition to higher rates of electron transport, heat dissipation acts as a photoprotective mechanism (Demmig-Adams and Adams 1992; Kato et al. 2003; Kitao et al. 2003, 2006b). Heat dissipation reduces the quantum yield of open PS II (F'_v/F'_m), and is defined as $1 - F'_v/F'_m$ (Demmig-Adams et al. 1995; Gilmore and Björkman 1995). *S. senanensis* likely has the highest heat dissipation ability under high

incident light among the three species tested, as indicated by its relatively low F'_v/F'_m values at high PPFD (Fig. 1c). Reflecting these differences in ETR and in heat dissipation, the magnitude of the excess energy (E) that was neither utilized nor dissipated in “shade plants” was smallest in *S. senanensis* (Fig. 2). Photoinactivation of PS II is considered to result from the excess energy (Demmig-Adams and Adams 1992; Osmond 1994; Niyogi 1999); this inactivation is linearly correlated with the magnitude of the excess energy, with a single proportion constant for plants that have varying capacities of photosynthesis and heat dissipation (Kato et al. 2003). In our study, the difference in the rate of excess light energy also reflected the difference in susceptibility to photoinhibition, as indicated by the decrease and recovery in predawn F_v/F_m values for the three species (Figs. 2, 4). In addition, avoidance of light-absorption through lower chlorophyll contents has been considered as one of photoprotective mechanisms (Hauvaux and Tardy 1999). However, the lower susceptibility to photoinhibition of *S. senanensis* compared with two broadleaved tree species cannot be the result of lower leaf absorptance of light, because absorptance of *S. senanensis* leaves was actually higher than those of two broadleaved tree species (Table 2). Though altering leaf angles is also a photoinhibition avoidance mechanism (Lovelock et al. 1994; Ishida et al. 2001), no visible leaf inclination differences were seen among the three species following gap formation.

Electron transport rate capacity is expected to be associated with area-based leaf N content (Evans 1996). *S. senanensis* had the highest N_{area} despite having similar N_{mass} , because its LMA, a leaf morphological trait, was particularly high (Table 2; Fig. 8). Similar findings have been reported for determinants of N_{area} in deciduous trees (Niinemets et al. 2004; Jones and Thomas 2007). The maintenance of high LMA under shade conditions (Table 2; Fig. 8a; *S. senanensis* > *Q. mongolica* > *A. mono*) apparently confers higher tolerance to sudden irradiance increases by avoiding photoinhibition (through maintaining a higher ETR capacity). This large LMA associated with higher A_{area} and ETR may be attributed to the life style of *S. senanensis*, which is an evergreen understory species in deciduous forests; this bamboo is capable of significant carbon uptake during periods when the upper forest canopy is leafless (Lei and Koike 1998). Our results suggest that the same properties also function in avoidance of photoinhibition following abrupt increase in light intensity after a windfall event.

In *S. senanensis*, which experienced the lowest photoinhibition in response to suddenly increased light intensity (Fig. 4), shade-grown leaves exposed to increased irradiation (“gap plants”) did not change photosynthetic capacity (ETR and A_{area} ; Figs. 5a, 7a), though N_{area} values

were reduced (Fig. 8b) in comparison to “shade plants”. In many broadleaf tree species, fully expanded shade-grown leaves are not able to acclimate to increasing light intensities (Naidu and DeLucia 1997; Yamashita et al. 2000; Oguchi et al. 2003). Our results suggest that this is true for shade-grown leaves of *S. senanensis*. Though N_{area} remained unchanged over the period of observation in “shade plants” of *Q. mongolica* and *A. mono*, N_{area} of *S. senanensis* “shade plants” increased significantly from Day 13 (data not shown) to Day 34 (t test; $P < 0.05$). The longer maturation period of *S. senanensis* perennial leaves cause this increase in N_{area} . The change in light conditions during *S. senanensis* leaf maturation might cause the N reallocation and affect the decrease in N_{area} of “gap plants” in comparison to “shade plants” (Fig. 8b).

Shade-grown seedlings of *Q. mongolica* had lower levels of photoinhibition than *A. mono* (Fig. 4). This field experiment result agrees with conclusions drawn from work on potted seedlings (Kitao et al. 2000, 2006a), which led to the characterization of *Q. mongolica* as a gap-dependent species and *A. mono* as a shade-tolerant one (Koike 1988). Photoinhibition is closely related to a decrease in q_p , i.e. an excess of excitation energy in PS II (Ögren 1994). The susceptibility to photoinhibition is considered to depend on the redox state of PS II measured as $1 - q_p$ (Ögren 1991; Öquist et al. 1993; Grey et al. 1996). *A. mono*, which had the largest decline in predawn F_v/F_m following gap formation (Fig. 4), had the lowest q_p at high irradiance (Fig. 1b). The lower ETR and q_p , and larger magnitude of excess energy at high irradiance (Figs. 1, 2) explain the higher susceptibility to photoinhibition in *A. mono*. One month following gap formation, q_p increased in *Q. mongolica* and *A. mono*, and F'_v/F'_m decreased in *A. mono* (Fig. 5); the relationships between magnitude of excess energy and absorbed PPFD changed to *S. senanensis*, and the rate of excess energy decreased (Fig. 6). These results were obtained at $600 \mu\text{mol m}^{-2} \text{s}^{-1}$ PPFD and we have no data under higher light conditions. Although *A. mono* had the lowest recovery rate in predawn F_v/F_m , we suggest that, at 1 month after gap formation, the two broadleaved tree species may have partial acclimation of photosynthetic activity to higher light conditions under newly formed canopy gaps.

Leaves developed after gap formation often have full physiological and morphological acclimation to the high light environment (Kamaluddin and Grace 1992; Pearcy 1994; Uemura et al. 2000; Yamashita et al. 2000). *S. senanensis* (which had the highest tolerance to photoinhibition), while *Q. mongolica* and *A. mono* were able to produce new leaves that may be expected to acclimate to high irradiance in the following year. In addition, *Q. mongolica* and *A. mono* increase shoot elongation rates when the environment is favorable for growth (Seiwa and Kikuzawa

1996; Koike et al. 1997). Since *S. senanensis* does not grow taller than about 1 m, “gap plants” of *Q. mongolica* and *A. mono* might break through the *S. senanensis* crown layer before the density of the bamboo culms increases in the year following gap formation. In addition, species with long-lived leaves have a much narrower range of photosynthetic plasticity than species with short-lived leaves (Lovelock et al. 1998). In our study site, the *S. senanensis* population regained size vegetatively, but has not yet recovered its original density after numerous patches died off in 1995 (Abe et al. 2003). In addition, when understory bamboo density was low, seedlings of broadleaf tree species sprouted up. When this happens, broadleaved tree species might be able to regenerate if they elongate through the canopy layer of *S. senanensis*. Density of *Sasa* and seedling sizes of broadleaved tree species when a disturbance occurs may influence subsequent regeneration success.

In conclusion, when large canopy gaps are created by typhoons in the late growing season, *S. senanensis* is less susceptible to photoinhibition (caused by increased light intensities) than two of the main broadleaf tree species, *Q. mongolica* and *A. mono*, in Japanese deciduous forests. Higher area-based net CO₂ assimilation rates and electron transport capacity, together with high LMA and N_{area} may contribute to the superior performance of *S. senanensis*. Previous studies showed that dwarf *Sasa* bamboos often became dominant in sun-exposed locations after large disturbances to the forest ecosystem (Ishizuka et al. 1998; Noguchi and Yoshida 2004). The reduced degree of photoinhibition in *S. senanensis*, which we demonstrated under field conditions, may be considered as one of the factors accounting for the success of this species in gap dynamics. However, other competitive abilities among species, like capacity for vegetative propagation, are likely more important than photoinhibition in determining persistence after disturbance (Lovelock et al. 1994).

Acknowledgments We thank Dr. S. Iida and Dr. S. Abe for their kind permission to use their study site, and Mrs. H. Taoka and Mr. K. Mima for assistance. We also thank Dr. T. Koike for helpful comments. This study was supported in part by a Grant-in-Aid (Research Project for Parameterization of Terrestrial Ecosystem for Integrated Global Modeling, Research Revolution 2002) from Japan’s Ministry of Education, Culture, Sports, Science and Technology, and by the Program for Promotion of Basic and Applied Researches for Innovations in Bio-oriented Industry (BRAIN).

References

- Abe S, Tanouchi H, Utsugi H, Iida S (2003) Mice and *Sasa* interaction on natural regeneration of Japanese oak (*Quercus crispula*). Trans Meeting Hokkaido Branch Jpn For Soc 51:61–63 (in Japanese)
- Abe M, Miguchi H, Makita A, Nakashizuka T (2005) Short-term changes affecting regeneration of *Fagus crenata* after the simultaneous death of *Sasa kurilensis*. J Veg Sci 16:49–56
- Baroli I, Melis A (1998) Photoinhibitory damage is modulated by the rate of photosynthesis and by the photosystem II light-harvesting chlorophyll antenna size. Planta 205:288–296
- Bazzaz FA (1996) Plants in changing environments: linking physiological, population and community ecology. Cambridge University Press, Cambridge
- Beaudet M, Brisson J, Gravel D, Messier C (2007) Effect of a major canopy disturbance on the coexistence of *Acer saccharum* and *Fagus grandifolia* in the understorey of an old-growth forest. J Ecol 95:458–467
- Demmig-Adams B, Adams WW III (1992) Photoprotection and other responses of plants to high light stress. Annu Rev Plant Physiol Plant Mol Biol 43:599–626
- Demmig-Adams B, Adams WW III, Logan BA, Verhoeven AS (1995) Xanthophyll cycle-dependent energy dissipation and flexible PS II efficiency in plants acclimated to light stress. Aust J Plant Physiol 22:249–260
- Demmig-Adams B, Adams WW III, Baker DH, Logan BA, Bowling DR, Verhoeven AS (1996) Using chlorophyll fluorescence to assess the fraction of absorbed light allocated to thermal dissipation of excess excitation. Physiol Plant 98:253–264
- Evans JR (1996) Developmental constraints on photosynthesis: effects of light and nutrition. In: Baker NR (ed) Photosynthesis and the environment. Kluwer, Dordrecht, pp 281–304
- Genty B, Briantais J-M, Baker NR (1989) The relationship between the quantum yield of photosynthetic electron transport and quenching of chlorophyll fluorescence. Biochim Biophys Acta 990:87–92
- Gilmore AM, Björkman O (1995) Temperature-sensitive coupling and uncoupling of ATPase-mediated, nonradiative energy dissipation: similarities between chloroplasts and leaves. Planta 197:646–654
- Grey RG, Savith LV, Ivanov AG, Huner NPA (1996) Photosystem II excitation pressure and development of resistance to photoinhibition. Plant Physiol 110:61–71
- Hauvaux M, Tardy F (1999) Loss of chlorophyll with limited reduction of photosynthesis as an adaptive response of Syrian barley landrace to high-light and heat stress. Aust J Plant Physiol 26:569–578
- Hiura T, Sano J, Konno Y (1996) Age structure and response to fine-scale disturbances of *Abies sachalinensis*, *Picea jezoensis*, *Picea glehnii*, and *Betula ermanii* growing under the influence of a dwarf bamboo understory in northern Japan. Can J For Res 26:289–297
- Iida S (2004) Indirect negative influence of dwarf bamboo on survival of *Quercus* acorn by hoarding behavior of wood mice. For Ecol Manag 202:257–263
- Ishida A, Nakano T, Uemura A, Yamashita N, Tanabe H, Koike N (2001) Light-use properties in two sun-adapted shrubs with contrasting canopy structures. Tree Physiol 21:497–504
- Ishizuka M, Toyooka H, Osawa A, Kushima H, Kanazawa Y, Sato A (1998) Secondary succession following catastrophic windthrow in a boreal forest in Hokkaido, Japan: the timing of the tree establishment. J Sustain For 6:367–388
- Ishizuka S, Sakata T, Sawata S, Ikeda S, Takenaka C, Tamai N, Sakai H, Shimizu T, Kan-Na K, Onodera S, Tanaka N, Takahashi M (2006) High potential for increase in CO₂ flux from forest soil surface due to global warming in cooler areas of Japan. Ann For Sci 63:537–546
- Jones TA, Thomas SC (2007) Leaf-level acclimation to gap creation in mature *Acer saccharum* trees. Tree Physiol 27:281–290

- Kamaluddin M, Grace J (1992) Photoinhibition and light acclimation in seedlings of *Bischofia javanica*, a tropical forest tree from Asia. *Ann Bot* 69:47–52
- Kato MC, Hikosaka K, Hirotsu N, Makino A, Hirose T (2003) The excess light energy that is neither utilized in photosynthesis nor dissipated by photoprotective mechanisms determines the rate of photoinactivation in photosystem II. *Plant Cell Physiol* 44:318–325
- Kitao M, Lei TT, Koike T, Tobita H, Maruyama Y (2000) Susceptibility to photoinhibition of three deciduous broadleaf tree species with different successional traits raised under various light regimes. *Plant Cell Environ* 23:81–89
- Kitao M, Utsugi H, Kuramoto S, Tabuchi R, Fujimoto K, Lihpai S (2003) Light-dependent photosynthetic characteristics indicated by chlorophyll fluorescence in five mangrove species native to Pohnpei Island, Micronesia. *Physiol Plant* 117:376–382
- Kitao M, Lei TT, Koike T, Tobita H, Maruyama Y (2006a) Tradeoff between shade adaptation and mitigation of photoinhibition in leaves of *Quercus mongolica* and *Acer mono* acclimated to deep shade. *Tree Physiol* 26:441–448
- Kitao M, Yoneda R, Tobita H, Matsumoto Y, Maruyama Y, Arifin A, Azani AM, Muhamad MN (2006b) Susceptibility to photoinhibition in seedlings of six tropical fruit tree species native to Malaysia following transplantation to a degraded land. *Trees* 20:601–610
- Koike T (1988) Leaf structure and photosynthetic performance as related to the forest succession of deciduous broad-leaved trees. *Plant Species Biol* 3:77–87
- Koike T, Miyashita N, Toda H (1997) Effects of shading on leaf structural characteristics in successional deciduous broadleaved tree seedlings and their silvicultural meaning. *For Resour Environ* 35:9–25
- Krause GH (1994) Photoinhibition induced by low temperatures. In: Baker NR, Bowyer JR (eds) *Photoinhibition of photosynthesis from molecular mechanisms to the field*. Bios Scientific Publishers, Oxford, pp 331–348
- Krause GH, Weis E (1991) Chlorophyll fluorescence and photosynthesis: the basics. *Annu Rev Plant Physiol Plant Mol Biol* 42:313–349
- Krause GH, Virgo A, Winter K (1995) High susceptibility to photoinhibition of young leaves to tropical forest trees. *Planta* 197:583–591
- Krause GH, Koroleva OY, Dalling JW, Winter K (2001) Acclimation of tropical tree seedlings to excessive light in simulated tree-fall gaps. *Plant Cell Environ* 24:1345–1352
- Lei TT, Koike T (1998) Functional leaf phenotypes for shaded and open environments of a dominant dwarf bamboo (*Sasa senanensis*) in northern Japan. *Int J Plant Sci* 159:812–820
- Leitsch J, Schnettger B, Critchley C, Krause GH (1994) Two mechanisms of recovery from photosystem II related and unrelated to D1-protein turnover. *Planta* 194:15–21
- Long SP, Humphries S, Falkowski PG (1994) Photoinhibition of photosynthesis in nature. *Annu Rev Plant Physiol Plant Mol Biol* 45:633–662
- Lovelock CE, Jebb M, Osmond CB (1994) Photoinhibition and recovery in tropical plant species: response to disturbance. *Oecologia* 97:297–307
- Lovelock CE, Kursar TA, Skillman JB, Winter K (1998) Photoinhibition in tropical forest understory species with short- and long-lived leaves. *Funct Ecol* 12:553–560
- Markwell J, Osterman JC, Mitchell JL (1995) Calibration of the Minolta SPAD-502 leaf chlorophyll meter. *Photosynth Res* 46:467–472
- Naidu SL, DeLucia EH (1997) Acclimation of shade-developed leaves on saplings exposed to late-season canopy gaps. *Tree Physiol* 17:367–376
- Nakashizuka T (1988) Regeneration of beech (*Fagus crenata*) after the simultaneous death of undergrowing dwarf bamboo (*Sasa kurilensis*). *Ecol Res* 3:21–35
- Narukawa Y, Yamamoto S (2002) Effects of dwarf bamboo (*Sasa* sp.) and forest floor microsites on conifer seedling recruitment in a subalpine forest, Japan. *For Ecol Manag* 163:61–70
- Niinemetts Ü, Kull O, Tenhunen JD (2004) Within-canopy variation in the rate of development of photosynthetic capacity is proportional to integrated quantum flux density in temperate deciduous trees. *Plant Cell Environ* 27:293–313
- Niyogi KK (1999) Photoprotection revisited: genetic and molecular approaches. *Annu Rev Plant Physiol Plant Mol Biol* 50:333–359
- Noguchi M, Yoshida T (2004) Tree regeneration in partially cut conifer-hardwood mixed forest in northern Japan: roles of establishment substrate and dwarf bamboo. *For Ecol Manag* 190:335–344
- Ögren E (1991) Prediction of photoinhibition of photosynthesis from measurements of fluorescence quenching components. *Planta* 184:538–544
- Ögren E (1994) The significance of photoinhibition for photosynthetic productivity. In: Baker NR, Bowyer JR (eds) *Photoinhibition of photosynthesis from molecular mechanisms to the field*. Bios Scientific Publishers, Oxford, pp 433–447
- Oguchi R, Hikosaka K, Hirose T (2003) Does the photosynthetic light-acclimation need change in leaf anatomy? *Plant Cell Environ* 26:505–512
- Oguchi R, Hikosaka K, Hirose T (2005) Leaf anatomy as a constraint for photosynthetic acclimation: differential responses in leaf anatomy to increasing growth irradiance among three deciduous trees. *Plant Cell Environ* 28:916–927
- Öquist G, Hurry VM, Huner NPA (1993) The temperature dependence of the redox state of Q_A and the susceptibility of photosynthesis to photoinhibition. *Plant Physiol Biochem* 31:683–691
- Osmond CB (1994) What is photoinhibition? Some insights from comparisons of shade and sun plants. In: Baker NR, Bowyer JR (eds) *Photoinhibition of photosynthesis from molecular mechanisms to the field*. Bios Scientific Publishers, Oxford, pp 1–24
- Pearcy RW (1994) Photosynthetic response to sunflecks and light gaps: mechanisms and constraints. In: Baker NR, Bowyer JR (eds) *Photoinhibition of photosynthesis from molecular mechanisms to the field*. Bios Scientific Publishers, Oxford, pp 255–271
- Pearcy RW, Sims DA (1994) Photosynthetic acclimation to changing light environments: scaling from the leaf to the whole plant. In: Caldwell MM, Pearcy RW (eds) *Exploitation of environmental heterogeneity by plants: ecophysiological processes above- and belowground*. Academic Press, San Diego, pp 145–174
- SAS Institute (2003) *JMP: statistics and graphics guide*, version 5.1. SAS Institute, Cary
- Schreiber U, Bilger W, Neubauer C (1994) Chlorophyll fluorescence as a noninvasive indicator for rapid assessment of in vivo photosynthesis. In: Schulze E-D, Caldwell MM (eds) *Ecophysiology of photosynthesis*. Springer, Berlin, pp 49–70
- Seiwa K, Kikuzawa K (1996) Importance of seed size for the establishment of seedlings of five deciduous broad-leaved tree species. *Vegetation* 123:51–64
- Shimizu M, Ishida A, Tange T, Yagi H (2006) Leaf turnover and growth responses of shade-grown saplings of four *Shorea* rain forest species to a sudden increase in light. *Tree Physiol* 26:449–457
- Sims DA, Pearcy RW (1992) Response of leaf anatomy and photosynthetic capacity in *Alocasia macrorrhiza* (Araceae) to a transfer from low to high light. *Am J Bot* 79:449–455
- Takahashi K, Mitsuishi D, Uemura S, Suzuki JI, Hara T (2003) Stand structure and dynamics during a 16-year period in a sub-boreal

- conifer-hardwood mixed forest, northern Japan. *For Ecol Manag* 174:39–50
- Takao G, Utsugi H, Sasaki S, Iida S, Abe S, Tobita H (2005) Evaluation of windfall damages on a deciduous broadleaf forest using LIDAR. *J Jap Soc Photogramm Rem Sens* 44:18–21 (in Japanese)
- Tatewaki M (1958) Forest ecology of the islands of the north Pacific Ocean. *J Fac Agric Hokkaido Univ* 1:371–486
- Thiele A, Schirwitz K, Winter K, Krause GH (1996) Increased xanthophyll cycle activity and reduced D1 protein inactivation related to photoinhibition in two plant systems acclimated to excess light. *Plant Sci* 115:237–250
- Tobita H, Kitao M, Maruyama Y (2002) Seasonal changes in light conditions and chlorophyll *a* fluorescence in *Picea jezoensis* saplings under deciduous broad-leaved forest of northern Japan. *Trans Mtg Hokkaido Br Jpn For Soc* 50:11–13 (in Japanese)
- Uddling J, Gelang-Alfredsson J, Piikki K, Pleijel H (2007) Evaluating the relationship between leaf chlorophyll concentration and SPAD-502 chlorophyll meter readings. *Photosynth Res* 91:37–46
- Uemura A, Ishida A, Nakano T, Terashima I, Tanabe H, Matsumoto Y (2000) Acclimation of leaf characteristics of *Fagus* species to previous-year and current-year solar irradiances. *Tree Physiol* 20:945–951
- Umeki K, Kikuzawa K (1999) Long-term growth dynamics of natural forests in Hokkaido, northern Japan. *J Veg Sci* 10:815–824
- Utsugi H, Tobita H, Maruyama Y, Ishizuka M (2005) Spatial and seasonal variation in leaf morphology in a canopy of a deciduous forest in northern Japan. *Phyton* 45:245–251
- Wyka T, Robakowski P, Zytowski R (2007) Acclimation of leaves to contrasting irradiance in juvenile trees differing in shade tolerance. *Tree Physiol* 27:1293–1306
- Yamashita N, Ishida A, Kushima H, Tanaka N (2000) Acclimation to sudden increase in light favoring an invasive over native trees in subtropical islands, Japan. *Oecologia* 125:412–419